The role of 14q32 microRNAs in vascular remodelling

Welten, S.M.J.

Chapter 6

Inhibition of Mef2a enhances post-ischemic neovascularization via 14q32 microRNAs miR-329 and miR-494

Submitted to Molecular Therapy

SMJ Welten[1,2]

MR de Vries[1,2]

HAB Peters[1,2]

S Agrawal[3]

PHA Quax[1,2*]

AY Nossent[1,2*]

[*]Authors contributed equally to this work

[1]Department of Surgery and [2]Einthoven Laboratory for Experimental Vascular Medicine,

Leiden University Medical Center, Leiden, the Netherlands

[3]Idera Pharmaceuticals, Cambridge, MA, United States of America

Abstract

Improving the efficacy of neovascularization is a promising strategy to restore perfusion of ischemic tissues in patients with peripheral arterial disease. The 14q32 microRNA cluster is highly involved in neovascularization. The Mef2a transcription factor has been shown to induce transcription of the microRNAs within this cluster. In the present study, we examined the role of Mef2a inhibition on post-ischemic neovascularization, potentially via regulation of the 14q32 microRNA cluster.

We inhibited expression of Mef2a using gene silencing oligonucleotides (GSOs) in an *in vivo* hind limb ischemia model. Treatment with GSO-Mef2a clearly improved blood flow recovery within 3 days (44% recovery versus 25% recovery in control) and persisted until 14 days after ischemia induction (80% recovery versus 60% recovery in control). Animals treated with GSO-Mef2a showed increased arteriogenesis and angiogenesis in the relevant muscle tissues. Inhibition of Mef2a decreased expression of 14q32 microRNAs miR-329 ($p=0.026$) and miR-494 (trend, $p=0.06$), but not of other 14q32 microRNAs, nor of 14q32 pri-miR or pre-miR transcripts.

Our study demonstrates a novel function for Mef2a in post-ischemic neovascularization via indirect regulation of 14q32 microRNAs miR-329 and miR-494. Inhibition of Mef2a could be a promising therapeutic strategy to increase blood flow recovery in patients with peripheral arterial disease.

Introduction

Patients with peripheral arterial disease (PAD) suffer from reduced blood supply towards the extremities, caused by the build-up of obstructive atherosclerotic plaques in the arterial wall. Restoration of blood flow in these patients is imperative for the prevention of critical limb ischemia and limb loss. This can be accomplished by stimulating post-ischemic neovascularization, i.e. arteriogenesis and angiogenesis. Arteriogenesis, the outward remodelling of pre-existent collateral arterioles, is initiated upon increases in shear stress through the arterioles[1]. Angiogenesis is driven by ischemia and leads to sprouting of new capillaries from existing blood vessels into the ischemic tissue[2]. Both arteriogenesis and angiogenesis are multifactorial processes that involve for example the activation of endothelial cells (ECs), proliferation of vascular cell types (especially smooth muscle cells (SMCs)) and recruitment of immune cells.

MicroRNAs are short, non-coding RNA molecules that regulate the expression of their target genes at the post-transcriptional level[3]. Each microRNA has multiple target genes and microRNA-binding to a target messenger RNA downregulates the expression of that gene. The ability of microRNAs to target numerous genes makes them attractive targets for the regulation of multifactorial physiological processes. In the past decade, microRNAs have emerged as key regulators in the development and progression of cardiovascular disease[4-9]. Recently, we have shown the involvement of multiple microRNAs from a single microRNA cluster located on human chromosome 14q32 in post-ischemic neovascularization[10]. The 14q32 locus contains the largest known mammalian microRNA gene cluster and contains 54 microRNAs in humans (12F1 locus in mice, containing 61 microRNAs)[11]. In our previous study, we showed that inhibition of microRNAs miR-329, miR-487b, miR-494 and miR-495 from the 14q32 microRNA cluster led to improved blood flow recovery after induction of hind limb ischemia in mice[10]. Arteriogenesis and angiogenesis were both increased in respectively the adductor and soleus muscles of these mice. Myocyte Enhancer Factor 2a (Mef2a) was confirmed as a target gene of miR-329 and Mef2a expression was upregulated in the ligated hind limb after miR-329 inhibition. Interestingly, MEF2A itself was reported to target miR-329 and the other 14q32 microRNAs[12]. Several studies reported transcriptional regulation of the 14q32 microRNA cluster by the MEF2 family of transcription factors and in particular by MEF2A[12-14].

The MEF2 family of transcription factors consists of four members, namely MEF2A, -B, -C and –D. Although mainly studied for their role in muscle development and differentiation, MEF2 family members are also expressed in ECs and vascular SMCs[15, 16]. MEF2A and MEF2C are the predominant isoforms expressed in vascular cells. In ECs, MEF2 proteins have been shown to control vascular integrity by promoting EC survival whereas in SMCs, MEF2 proteins are expressed in cells with an activated phenotype and control differentiation of SMCs[17, 18]. Moreover, inhibition of MEF2A induced phenotypic switching of vascular SMCs, leading to proliferation and migration of these cells[19].

The aim of this study was to evaluate the effect of Mef2a inhibition on post-ischemic blood flow recovery. We hypothesized that Mef2a could act as a novel switch in neovascularization via regulation of 14q32 microRNAs. We show here that inhibition of Mef2a, via subsequent inhibition of 14q32 microRNAs miR-329 and miR-494, but not other 14q32 microRNAs, indeed improves post-ischemic

blood flow recovery *in vivo*.

Methods

Mef2a inhibitors

Gene silencing oligonucleotides (GSOs) were designed with reverse complementarity to the murine Mef2a target mRNA sequence and synthesized at Idera Pharmaceuticals (Cambridge, MA, USA)[23]. As a negative control, a scrambled sequence was used, designed not to target any known murine mRNA. GSOs were made up of two single-stranded DNA strands, which were 2'O-methylated. The two DNA strands were linked together at their 5'ends by a phosphothioate-linker in order to prevent Toll-like receptor mediated immune activation. Sequences of Mef2a GSOs are given in Figure 1.

Hind limb ischemia model

This study was performed in accordance with Dutch government guidelines and the Directive 2010/63/EU of the European Parliament. All experiments were approved by the committee on animal welfare of the Leiden University Medical Center (Leiden, the Netherlands. Approval reference number 12029). C57Bl/6 male mice, aged 8 to 12 weeks (Harlan) were housed in groups of 4 or 5 mice with free access to water and regular chow. For Mef2a-inhibition experiments, mice were given intraperitoneal (i.p) injections of 1 mg (~40 mg/kg) GSO in PBS or PBS alone at 10, 7, 4 days and directly before surgery and at 3, 7 and 10 days after surgery. Mice were anesthetized by i.p. injection of midazolam (8 mg/kg, Roche Diagnostics), medetomidine (0.4 mg/kg, Orion) and fentanyl (0.08 mg/kg, Janssen Pharmaceuticals). Unilateral hind limb ischemia was induced by electrocoagulation of the left femoral artery proximal to the superficial epigastric artery and proximal to the bifurcation of the popliteal and saphenous artery (double ligation model)[24]. After surgery, anaesthesia was antagonized with flumazenil (0.7 mg/kg, Fresenius Kabi), atipamezole (3.3 mg/kg, Orion) and buprenorphine (0.2 mg/kg, MSD Animal Health).

Laser Doppler perfusion measurements

Blood flow recovery to the ligated hind limb was measured over time using Laser Doppler Perfusion Imaging (LDPI) (Moor Instruments) before and directly after surgery and at at 3, 7, 10 and 14 days after surgery. For LDPI measurements, mice were anesthetized by i.p. injection of midazolam (8 mg/kg, Roche Diagnostics) and medetomidine (0.4 mg/kg, Orion). Before each measurement, mice were placed in a double glazed pot, perfused with water at 37°C for 5 minutes. After LDPI, anaesthesia was antagonized by subcutaneous injection of flumazenil (0.7 mg/kg, Fresenius Kabi) and atipamezole (3.3 mg/kg, Orion). LDPI measurements in the ligated paw were normalized to measurements of the unligated paw, as internal control. After the last LDPI measurement at day 14, analgesic fentanyl (0.08 mg/kg, Janssen Pharmaceuticals) was administered subcutaneously and mice were sacrificed via cervical dislocation. The adductor, gastrocnemius and soleus muscles were harvested and either snap-frozen or fixed in 4% PFA.

Cell culture

Primary murine smooth muscle cells. Primary murine smooth muscle cells were isolated from mouse aortae of C57Bl/6 mice. Aortae were cut into small pieces and embedded on gelatin coated 6-well plates. Culture medium was added to the wells with aortic fragments (DMEM (Invitrogen, GIBCO), 10% heat inactivated fetal bovine serum (PAA), 1% penicillin/streptomycin). Outgrowth of smooth muscle cells occurred within one week, after which cells were passed using Trypsin-EDTA (Sigma) and transferred to fresh 6-well plates. Smooth muscle cells were characterized by positive α-smooth muscle actin staining as described previously[10]. Cells were cultured at 37°C in a humidified 5% CO_2 environment.

3T3 cells. 3T3 cells were cultured at 37ºC in a humidified 5% CO_2 environment. Culture medium consisted of DMEM GlutaMAX (Gibco) supplemented with 10% heat inactivated fetal bovine serum (PAA) and 1% penicillin/streptomycin (PAA). Culture medium was refreshed every 2-3 days. Cells were passed using trypsin-EDTA (Sigma) at 90% confluency.

In vitro GSO mediated inhibition of Mef2a expression

For GSO experiments, murine smooth muscle cells were plated at 50.000 cells per well of a 12-well plate. After 24 hrs, GSOs against

Mef2a were added to the culture media at a concentration of 10ng/µl for 48 hrs. After 48 hrs, cells were washed with PBS and TRIzol (Invitrogen) was added to the cells for RNA isolation.

rt/qPCR

mRNA rt/qPCR. Adductor and gastrocnemius muscles from 14 days after surgery were homogenized by grounding with a pestle and mortar in liquid nitrogen. Total RNA was isolated using a standard TRIzol-chloroform extraction protocol. RNA concentration and purity were determined by nanodrop (Nanodrop Technologies). RNA was reverse transcribed using high-capacity RNA to cDNA RT kits (Life Technologies, Foster City, CA, USA). Relative quantitative mRNA PCR was performed on reverse transcribed cDNA using Mef2a Taqman gene expression assays. For quantification of pri-miR and pre-miR levels of microRNAs, SYBR green dye (Qiagen) was used and primers were designed using Primer3. Sequences of primers are listed in Supplementary Table 1. qPCRs were run on a 7900HT Fast Real-Time PCR system (Applied Biosystems), and amplification efficiencies were checked by standard curves. Data were normalized using a stably expressed endogenous control (HPRT for Mef2a quantification, snRNA-U6 for pri-miR and pre-miR quantification).

microRNA rt/qPCR. microRNA quantification was performed using Taqman microRNA assays (Applied Biosystems) according to manufacturer's protocol. Relative quantitative PCR was performed on the Viia7 system (Applied Biosystems) and amplification efficiencies were checked by standard curves. Data were normalized using a stably expressed endogenous control (mmu-let-7c), as previously described[25].

Immunohistochemistry

CD31. Six µm thick fresh-frozen cross-sections of soleus muscle were fixed in ice-cold acetone and stained with anti-CD31 (BD Pharmingen). Sections were counterstained with hematoxylin. Quantification of CD31 positive area was performed on sections photographed randomly (six representative images per muscle per mouse, ten animals per group) using image analysis (Image J 1.48v, NHI, USA), as described previously[26].

α-SMA, CD31 and CD45 triple staining. Five µm thick paraffin-embedded cross-sections of adductor muscle were re-hydrated and antigen retrieval was performed using citrate buffer. Smooth muscle cells were stained using primary antibodies against α-smooth muscle actin (α-SMA, DAKO), endothelial cells were stained with CD31 antibodies (BD Pharmingen) and leukocytes were stained using CD45 antibodies (Abcam). Alexa Fluor 647, Alexa Fluor 488 and Alexa Fluor 594 antibodies (Life Technologies and Invitrogen (Alexa Fluor 594)) were used to visualize smooth muscle cells, endothelial cells and leukocytes respectively. Finally, sections were mounted in Fluoroshield with DAPI (Sigma-Aldrich). The Pannoramic MIDI digital slide scanner (3DHistech) was used to create high resolution images of the adductor muscles. Snapshots were taken using the Pannoramic viewer software (3DHistech) with 20x magnification. The amount and size of α-SMA positive collaterals was measured using Image J (Image J 1.48v, NHI, USA).

MEF2A. Five µm thick paraffin-embedded cross-sections of adductor muscle were re-hydrated and endogenous peroxidase activity was blocked. Antigen retrieval was performed with Tris-EDTA (pH 9.0) at 100°C for 10 minutes. Adductor muscles were stained with Anti-MEF2A antibodies (Abcam, ab86755) to visualize MEF2A expression and counterstained with haematoxylin.

Western Blot analysis

Immunoblotting was performed to quantify MEF2A expression *in vivo*. Homogenized adductor muscle tissue of GSO-control (n=2) and GSO-Mef2a (n=2) treated animals were lysed on ice for 30 minutes with lysis buffer. Lysates were briefly centrifuged to remove debris. Equal amounts of protein (20 µg per sample) were loaded onto a PAGE minigel (Mini-PROTEAN TGX precast gel, Biorad) and run at 70V for 10 min and subsequently at 120V for 90 min. Fractionated tissue extracts were transferred to a nitrocellulose membrane using a transfer apparatus according to the manufacturer's protocol (Bio-Rad). Incubation with primary rabbit anti-MEF2A antibody (Abcam, ab86755 1:100) was followed by incubation with HRP-conjugated secondary antibody goat anti-rabbit IgG (CST7074, Cell Signalling Technology). Signals were visualized using the SuperSignal ELISA Pico chemiluminescent substrate (ThermoScientific). Blots were stripped for 15 min using Restore Stripping Buffer (ThermoScientific) and incubated with anti-Actin (C-11) (SC1615, Santa-Cruz) for normalization. The proportional expression of MEF2A per lane was normalized against the proportional expression of Actin per lane (Biorad Image Lab Software 5.2.1).

Aortic Ring assay

Mouse aortic ring assays were performed as described previously[27]. In brief, the thoracic aorta was removed from 8 to 10-week old mice and transferred to a 15 mL tube containing Opti-MEM (Gibco). Surrounding fat and branching vessels were carefully removed and aortas were flushed with Opti-MEM (Gibco). Collagen Type I (Millipore) was diluted to a final concentration of 1mg/ml with DMEM (Gibco) and pH was adjusted with 5N NaOH. 96-well plates were coated with 75 µl collagen matrix. After serum starvation overnight in Opti-MEM, aortic rings (0.5 to 1 mm) were transferred to the 96-well plate and after 1 hour, 150 µl Opti-MEM supplemented with 2.5% FBS (PAA, Austria), penicillin-streptomycin (PAA, Austria), 30ng/ml VEGF (Millipore) and GSOs (15ng/ul) was added to each well. Microvessel outgrowth was quantified after 5 days by live phase-contrast microscopy (Axiovert 40C, Carl Zeiss). Starting from a specific point on the ring, each microvessel emerging from the ring was counted as a sprout and individual branches arising from each microvessel counted as a separate sprout, working around the ring clockwise.

RNA Binding Protein Immunoprecipitation

RNA binding protein immunoprecipitation (RIP) was performed using the EZMagna RIP kit (Millipore), according to manufacturer's instructions. 3T3 cells were grown to 90% confluency and lysed in complete RIP lysis buffer. Cell lysates were incubated with RIP buffer containing magnetic beads conjugated with antibodies against MEF2A (Abcam ab86755) and rabbit control IgG (Millipore PP64B). Before immunoprecipitation, 10% of cell lysate was taken and served as 10% input control. Next, samples were treated with proteinase K to digest protein and RNA was isolated using a standard TRIzol-chloroform extraction protocol.

Statistical analysis

Results are expressed as mean ± SEM. *In vitro* experiments were performed in triplicate and represent at least three independent experiments. Differences between groups were tested using student's t-tests. P values of <0.05 were considered statistically significant.

Results

Gene Silencing Oligonucleotide mediated inhibition of Mef2a expression

We tested several Gene Silencing Oligonucleotides (GSOs) *in vitro* for their capacity to inhibit Mef2a mRNA expression in murine primary smooth muscle cells (GSO-1, GSO-2, GSO-3 and GSO-4, Fig. 1A). Expression of Mef2a was significantly inhibited by GSO-2 (35% expression of control, p=0.0005) and GSO-3 (30% expression of control, p=0.0094), but not by treatment with GSO-1 or GSO-4 (Fig. 1B). For *in vivo* experiments, we selected GSO-3 for inhibition of Mef2a (GSO-Mef2a from here on) which gave the strongest downregulation of Mef2a expression.

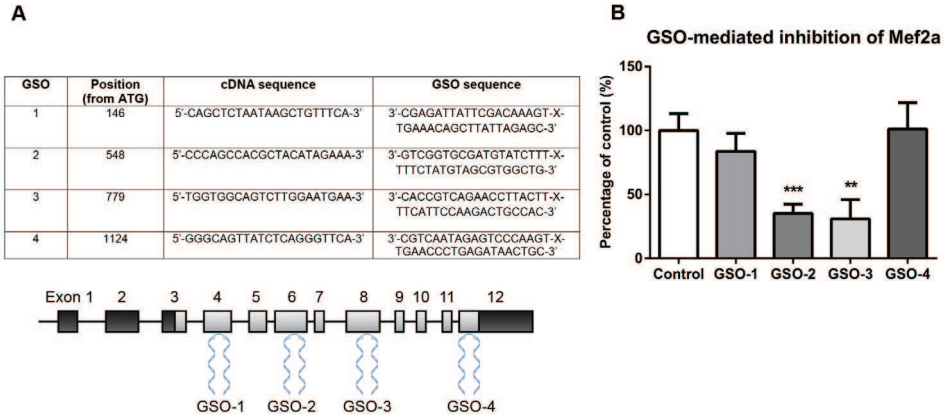

GSO	Position (from ATG)	cDNA sequence	GSO sequence
1	146	5'-CAGCTCTAATAAGCTGTTTCA-3'	3'-CGAGATTATTCGACAAAGT-X-TGAAACAGCTTATTAGAGC-3'
2	548	5'-CCCAGCCACGCTACATAGAAA-3'	3'-GTCGGTGCGATGTATCTTT-X-TTTCTATGTAGCGTGGCTG-3'
3	779	5'-TGGTGGCAGTCTTGGAATGAA-3'	3'-CACCGTCAGAACCTTACTT-X-TTCATTCCAAGACTGCCAC-3'
4	1124	5'-GGGCAGTTATCTCAGGGTTCA-3'	3'-CGTCAATAGAGTCCCAAGT-X-TGAACCCTGAGATAACTGC-3'

Figure 1. **Inhibition of Mef2a by Gene Silencing Oligonucleotides (GSOs). (A)** Four different GSOs were developed and tested for their capacity to inhibit Mef2a expression *in vitro*. GSOs were designed to target different exons on the murine Mef2a mRNA sequence. **(B)** Inhibition of Mef2a in primary murine vascular smooth muscle cells for 48 hrs by GSOs (10ng/µl). Mean expression levels, from at least 3 independent experiments, relative to HPRT and as percentage of GSO-Control are shown here (±SEM). **p<0.01, ***p<0,001.

In vivo inhibition of Mef2a using GSOs

Immunohistochemical staining of murine adductor muscle tissue demonstrated that MEF2A is expressed in this tissue, particularly in the nuclei of cells (Fig. 2A). Expression of Mef2a was measured in the adductor and gastrocnemius muscles of animals, 14 days after induction of ischemia, 4 days after the final GSO injection. Expression of Mef2a was downregulated in both adductor and gastrocnemius muscle tissue of GSO-Mef2a treated mice compared to control treated animals (Fig. 2B and 2C, respectively). Although inhibition of Mef2a was less strong than *in vitro* cell cultures, inhibition was highly significant (72% expression of control, p=0.00052 in the adductor and 78% expression of control, p<0.0001 in the gastrocnemius muscle). GSO-Mef2a treatment furthermore reduced MEF2A protein levels in the adductor muscle by 30% (Fig. 2D).

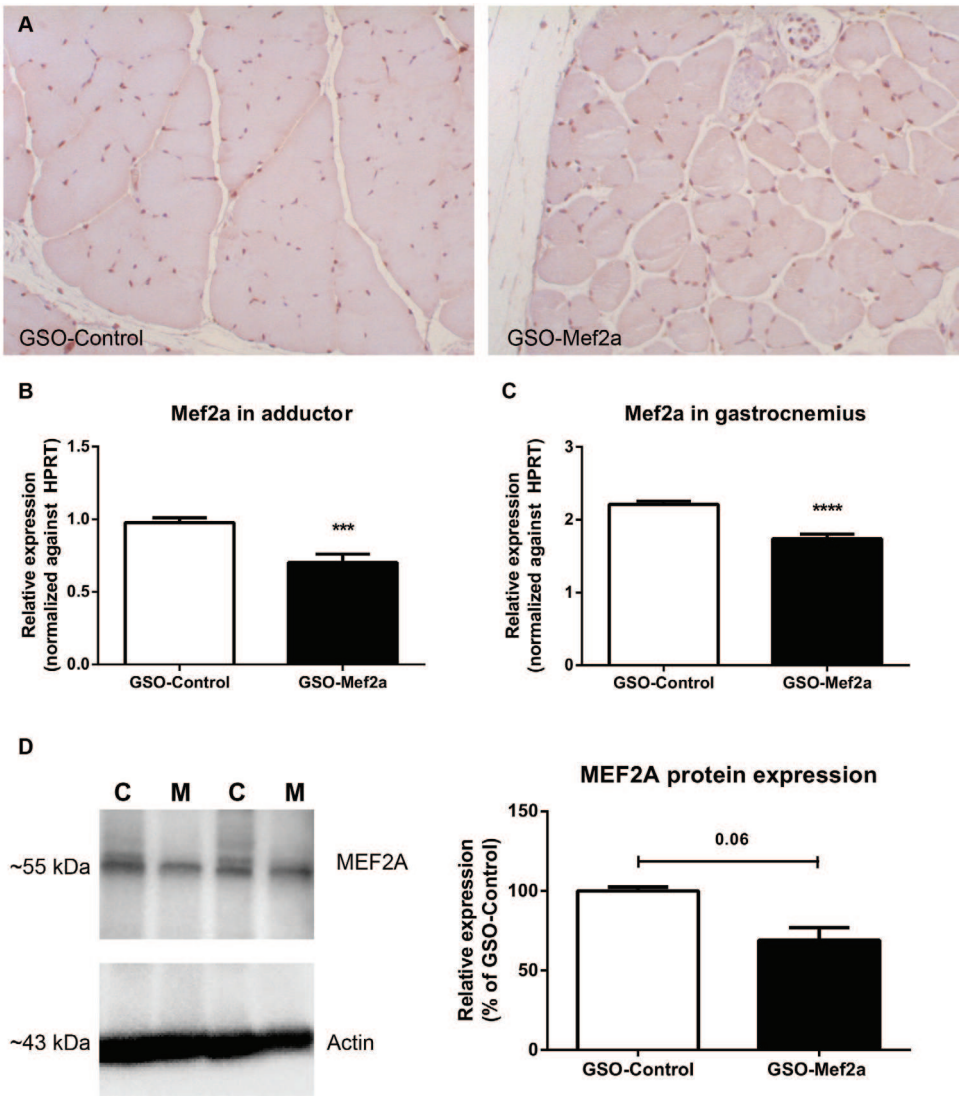

Figure 2. ***In vivo*** **inhibition of Mef2a by GSO-Mef2a**. **(A)** Immunohistochemical staining of MEF2A in the adductor muscle of GSO-Mef2a and GSO-Control treated mice. **(B)** Expression of Mef2a in the adductor muscle of C57Bl/6 mice treated with GSO-Mef2a or GSO-control, 14 days after double ligation of the left femoral artery. Per group, adductor muscle tissue of 10 animals was used. **(C)** Expression of Mef2a in the gastrocnemius muscle of C57Bl/6 mice treated with GSO-Mef2a or GSO-Control, 14 days after ischemia induction. Per group, gastrocnemius muscle tissue of 10 animals was used. Mean expression levels relative to HPRT are shown here (±SEM). **(D)** MEF2A and Actin protein expression and quantification in adductor muscle lysates of GSO-Mef2a (M) and GSO-Control (C) treated mice (n=2 animals per group). Mean expression as percentage of control is shown here (±SEM). ***p<0,001, ****p<0,0001.

Improved blood flow recovery upon Mef2a inhibition

The effect of Mef2a inhibition on blood flow recovery was evaluated at different time points after ligation of the femoral artery (pre-operative, post-operative, day 3, day 7, day 10 and day 14 after ischemia induction, Fig. 3). Already within 3 days after hind limb ischemia, animals injected with GSOs against Mef2a showed improved blood flow recovery (44% recovery in GSO-Mef2a animals versus

25% recovery in GSO-control animals, Fig. 3). This increase in perfusion persisted over time. At time of sacrifice, GSO-Mef2a treated animals showed 80% recovery in blood flow compared to 60% recovery of perfusion in GSO-Control treated animals.

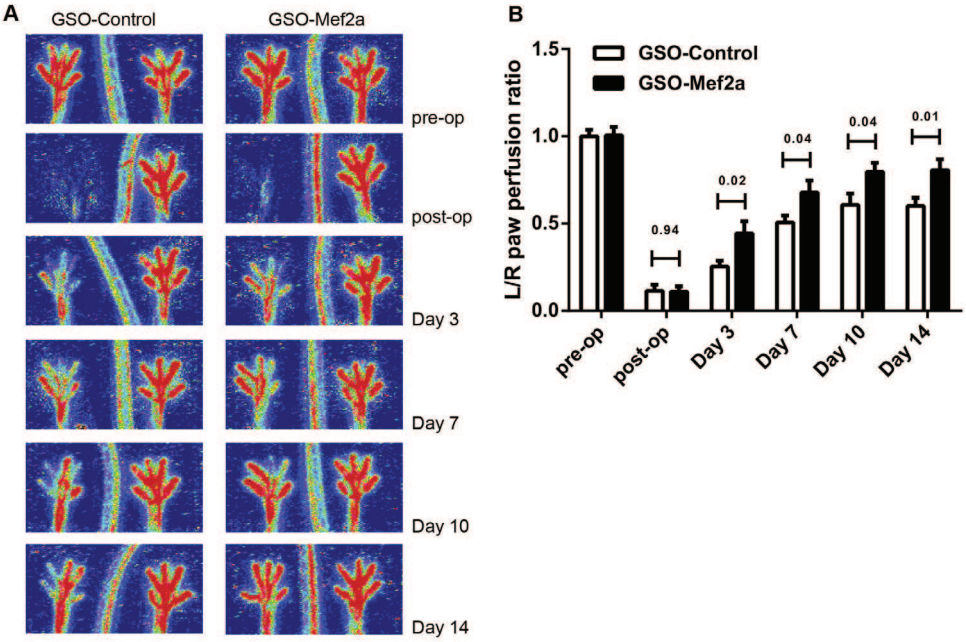

Figure 3. Blood flow recovery after *in vivo* Mef2a inhibition. (A) Laser Doppler perfusion images (LDPI) from paws of mice subjected to unilateral hind limb ischemia, showing blood flow recovery in these animals over time. **(B)** Quantification of LDPI measurements over time in mice (11 per group) treated with GSO-Mef2a or GSO-Control (1 mg per mouse injected i.p. at different time points as described in materials and methods). Data are calculated as the ratio of the left (ischemic) over the right (non-ischemic) paw and presented as mean ± SEM. P-values are shown for each time point.

In vivo inhibition of Mef2a increases arteriogenesis

Alpha smooth muscle actin (α-SMA$^+$) staining was used to visualize collateral vessels in the adductor muscle. Significant increases in arteriole diameters were observed between the left and right adductor muscles for GSO-Mef2a treated mice compared to GSO-control treated mice (increase in arteriole diameter in left over right adductor (LA/RA ratio) was 2.057 compared to LA/RA ratio of 1.16 in controls, p=0.0060, Fig. 4A). Both total α-SMA$^+$ area per section (LA GSO-Mef2a 846±99μm^2 vs RA GSO-Mef2a 404±37μm^2, p=0.00043 and LA GSO-Control 654±68μm^2 vs RA GSO-Control 480±27μm^2, p=0.05) as well as mean lumen area per α-SMA$^+$ collateral (LA GSO-Mef2a 342±25μm^2 vs RA GSO-Mef2a 170±9μm^2, p=0.0002 and LA GSO-Control 237±47μm^2 vs RA GSO-Control 217±18μm^2, p=0.54) were increased in the left adductor muscles of GSO-Mef2a treated animals compared to the right adductor muscles which was not the case for GSO-Control treated animals (Fig. 4B and 4C, respectively). Moreover, α-SMA$^+$ area per collateral was increased in the left adductor of GSO-Mef2a treated animals compared to controls (GSO-Mef2a 342±25μm^2 vs GSO-Control 237±47μm^2, p=0.03, Fig. 4C and representative images in Fig. 4D). The number of α-SMA$^+$ vessels between the left and right paw were similar in the GSO-Mef2a group (LA/RA ratio 1.04), whereas GSO-Control treated animals had more α-SMA$^+$ vessels

in the left compared to the right paw (LA/RA ratio 1.27, Fig. 4E). Arteriogenesis is the enlargement of pre-existing arterioles to form collateral arteries. Therefore, not the increase in number of collateral arteries but rather the increase in arteriole diameters demonstrate increased arteriogenesis in GSO-Mef2a treated mice. Furthermore, as an inflammatory environment facilitates extracellular matrix rearrangement and outward remodelling of collateral arterioles, we also looked at the number of inflammatory cells surrounding the collaterals. There was a trend towards an increase in the number of perivascular CD45$^+$ leukocytes around the remodelling collaterals of GSO-Mef2a treated animals compared to controls (64% increase compared to GSO-Control animals, p=0.09, Fig. 4F).

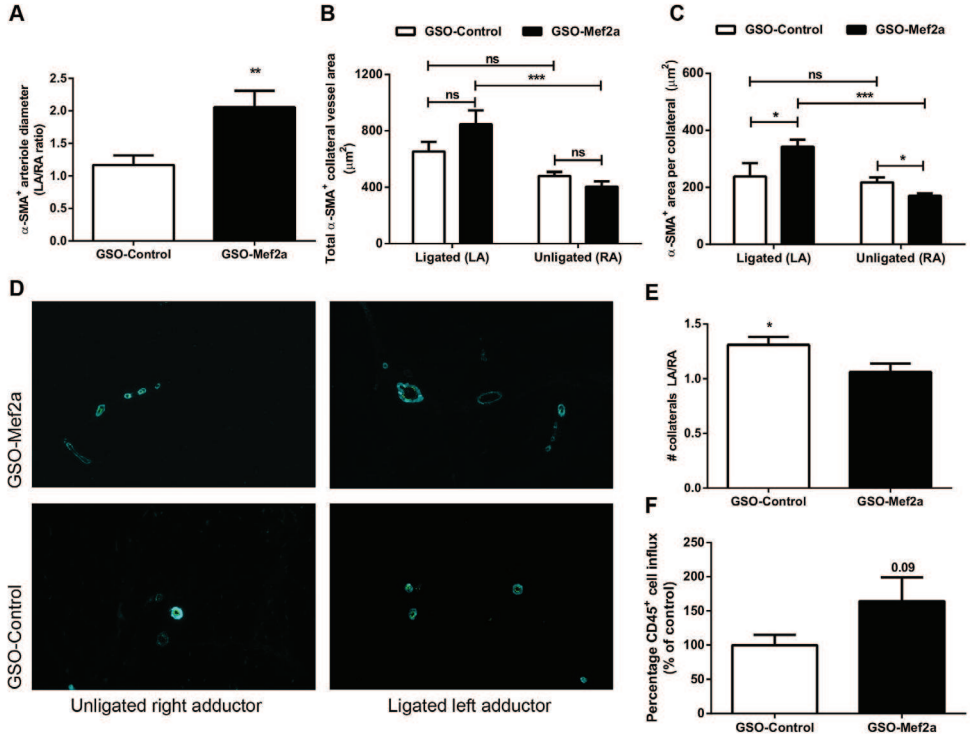

Figure 4. ***In vivo*** **arteriogenesis after Mef2a inhibition.** Immunofluorescence staining of paraffin-embedded adductor muscle group of C57Bl/6 mice treated with either GSO-control (n=11 animals) and GSO-Mef2a (n=10 animals), 14 days after ischemia induction, using anti-αSMA (turquoise) antibodies. **(A)** Quantification of the increase in diameter of α-SMA$^+$ arterioles between the left and the right adductor muscles of mice. **(B)** Total α-SMA$^+$ area per section as well as **(C)** mean lumen area per α-SMA$^+$ collateral are shown. **(D)** Representative images of α-SMA staining in unligated and ligated adductor muscle tissues of mice treated with GSO-Mef2a or GSO-Control. **(E)** Number of total collateral arterioles in left (ligated) over right (unligated) adductor muscles of mice. **(F)** Quantification of the number of CD45$^+$ cells around remodelling collateral arterioles in the adductor muscle of GSO-Control or GSO-Mef2a treated mice, 14 days after induction of ischemia. From each muscle, 8 representative images were used for quantification. Data are presented as mean ± SEM. *p<0.05, *p<0.001, ***p<0.0005.

In vivo angiogenesis upon Mef2a inhibition

Capillary formation was evaluated in the left (ischemic) and right (normoxic) soleus muscles of GSO-treated mice, 14 days after induction of ischemia. Muscle tissues were stained with anti-CD31 to visualize capillaries. Inhibition of Mef2a increased capillary formation in the soleus muscles of these mice (1.4 fold, p=0.04) compared to the soleus muscles of GSO-control treated mice (Fig. 5). We also

investigated the effect of Mef2a inhibition on *ex vivo* angiogenesis using aortic explants. GSO mediated inhibition of Mef2a led to a mild increase in the number of sprouts from aortic explants, compared to GSO-Control (Supplemental Fig. 1).

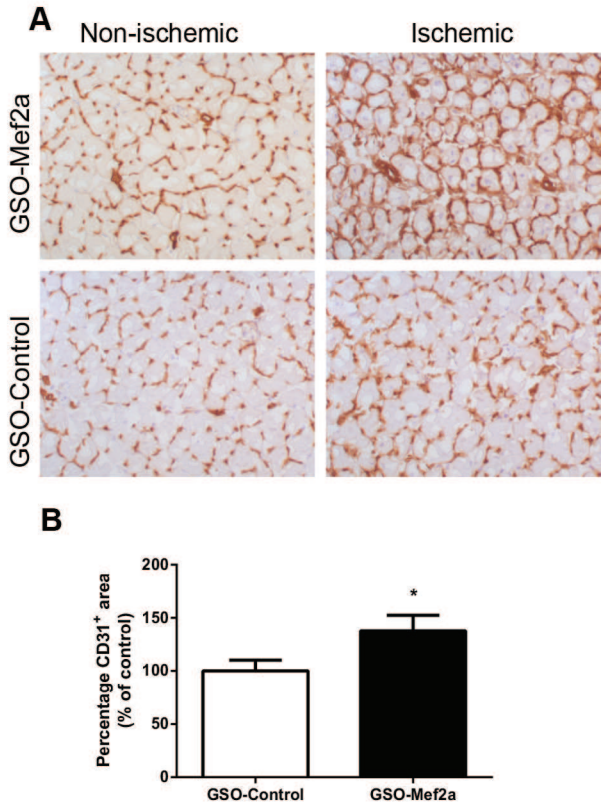

Figure 5. *In vivo* angiogenesis after Mef2a inhibition. (A) Representative images of CD31 staining in the right (non-ischemic) and left (ischemic) soleus muscles of C57Bl/6 mice treated with GSO-Mef2a (n=10 animals) or GSO-Control (n=11 animals). **(B)** Quantification of the capillary density in the soleus muscle, defined as the increase in $CD31^+$ area between left and right soleus muscles, shown as percentage relative to the increase in mice treated with GSO-Control. From each soleus muscle, 6 representative photographs were used for quantification. Data are presented as mean ± SEM. *p<0.05.

Mef2a targets miR-329 of the 14q32 microRNA cluster

We determined expression of 14q32 microRNAs miR-329, miR-487b, miR-494, miR-495 and miR-410 in the adductor muscles of GSO-Mef2a and GSO-Control treated mice. Inhibition of Mef2a led to significant downregulation of 14q32 microRNA miR-329 (Fig. 6A, p=0.0026) and a borderline significant downregulation of miR-494 (Fig. 6B, p=0.06). However, expression of 14q32 microRNAs miR-487b, miR-410 and miR-495 was not inhibited in animals treated with GSO-Mef2a (Fig. 6C-E). MicroRNAs are transcribed as primary microRNAs (pri-miRs) before being processed into pre-microRNAs (pre-miRs) and subsequently into mature microRNAs. To determine whether Mef2a does influence transcription of multiple 14q32 microRNAs, we also measured expression of the pri-miR transcripts and the intermediate pre-miRs in adductor muscle tissue of GSO-treated animals. No differences were

observed in pri-miR and pre-miR levels of any of the microRNAs between GSO-Mef2a and GSO-control treated animals, indicating that the regulation of mature miR-329 and miR-494 levels was indirect (Fig. 7).

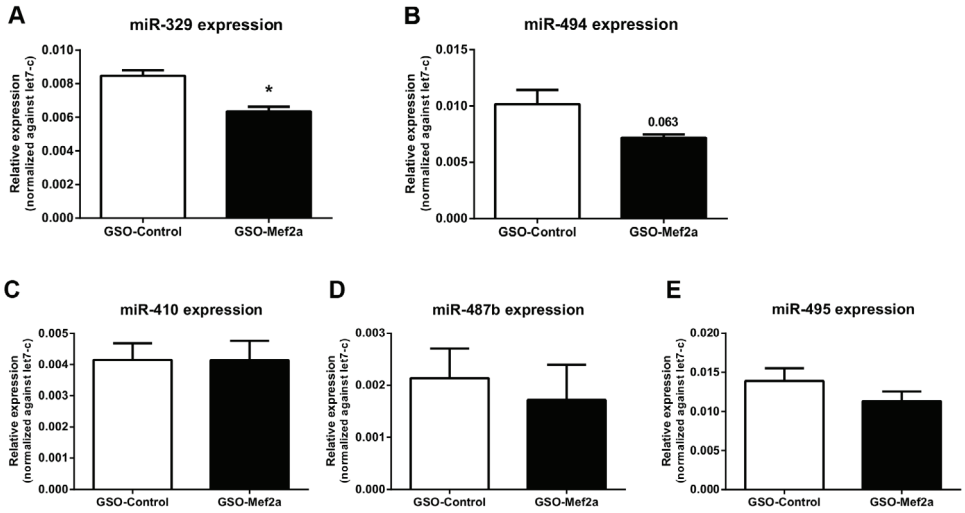

Figure 6. Regulation of 14q32 microRNA expression *in vivo*. Expression of 14q32 microRNAs miR-329 **(A)**, miR-494 **(B)**, miR-487b **(C)**, miR-410 **(D)** and miR-495 **(E)** in adductor muscle tissue of GSO-Mef2a or GSO-Control treated animals at 14 days after hind limb ischemia. Per group, adductor muscle tissue of 4 mice was used. Mean expression levels are shown here relative to expression of let-7c (±SEM). *p<0.05

Mef2a binds to the pri-miR transcript of 14q32 microRNA miR-494, but not miR-487b

To investigate whether Mef2a could regulate post-transcriptional processing of 14q32 microRNAs, we performed RNA binding protein immunoprecipitation (RIP) assays. RIP experiments on 3T3 cell lysates performed with anti-MEF2A antibodies demonstrated specific binding of MEF2A to the pri-miR-494 transcript, but not to the pri-miR-487b transcript (Supplemental Fig. 2). Expression of pri-miR-329 was too low to confirm or exclude MEF2A binding in these cells.

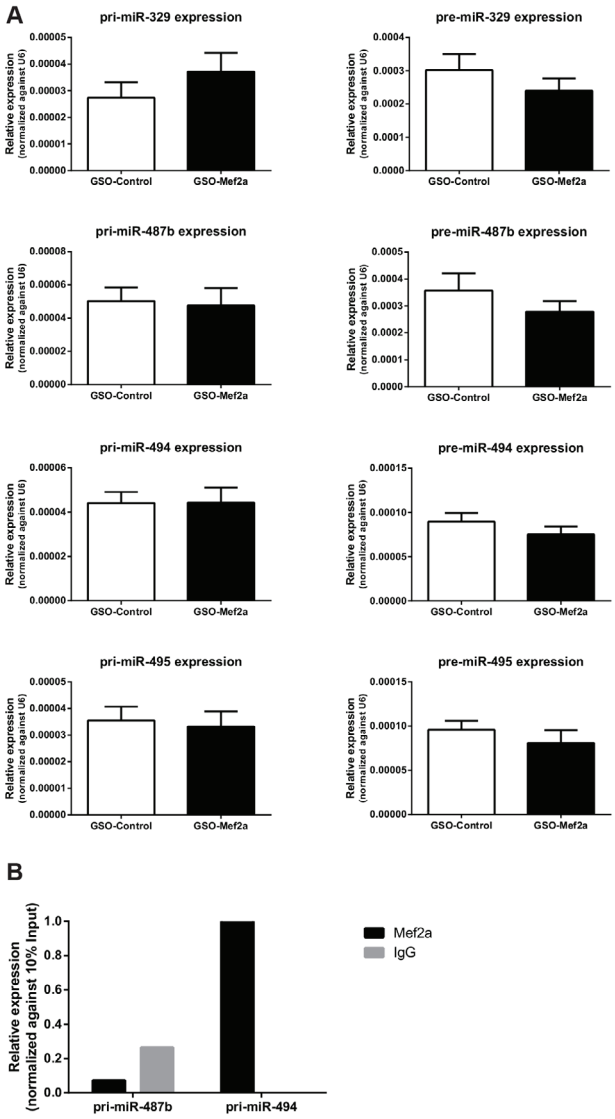

Figure 7. Regulation of 14q32 pri-miR and pre-miR expression *in vivo*. (A) Expression of pri-miR and pre-miR transcripts of 14q32 microRNAs miR-329, miR-487b, miR-494 and miR-495 in adductor muscle tissue of GSO-Mef2a or GSO-Control treated animals at 14 days after hind limb ischemia. Per group, adductor muscle tissue of 11 mice was used. Mean expression levels are shown here relative to expression of snRNA-U6 (±SEM). **(B)** RNA binding protein immunoprecipitation with either MEF2A antibodies or negative control rabbit IgG followed by rt/qPCR on pri-miR transcripts of 14q32 microRNAs miR-494 and miR-487b. Data are normalized against 10% input.

Discussion

We demonstrate here that the Mef2a transcription factor plays a role in post-ischemic neovascularization. Inhibition of MEF2A improved blood flow recovery in animals after unilateral ligation of the femoral artery. Previous reports have demonstrated the role of Mef2a in other forms of vascular remodelling as well. One study showed that the expression of MEF2 members Mef2a, Mef2b and Mef2d was increased in the neointima of rat carotid arteries after balloon injury[18]. In another study, overexpression of a dominant-negative mutant form of Mef2a reduced neointima formation, inhibited macrophage infiltration and decreased MCP1 expression upon wire injury in rats[20]. However, to our knowledge, a role of Mef2a in post-ischemic neovascularization is a completely novel finding.
We hypothesized that inhibition of Mef2a expression would improve post-ischemic neovascularization via subsequent downregulation of 14q32 microRNAs, as Mef2a was reported to control 14q32 microRNA expression and because we have previously shown that 14q32 microRNAs have anti-angiogenic and anti-arteriogenic functions[10, 12]. Inhibition of Mef2a in our study revealed decreased expression of 14q32 microRNA miR-329 and a trend towards decreased expression of miR-494, but not of several other 14q32 microRNAs studied here. Indeed, animals treated with GSO-Mef2a showed ~80% recovery of blood flow, 14 days after ischemia induction. However, this effect was not greater than inhibition of single 14q32 microRNAs miR-329 and miR-494, as inhibition of these microRNAs led to (nearly) complete restoration of blood flow within 7 and 10 days respectively.

In addition to the mature miR levels, we also determined expression levels of pri-miR transcripts and pre-miR intermediates of several 14q32 microRNAs. Pri-miR levels directly indicate the level of transcription of the 14q32 microRNA genes, which were expected to be influenced by the transcription factor Mef2a. Pre-miRs are an intermediate form of the microRNA transcript and changes in expression of the pri-miR to the pre-miR or from pre-miR to the mature microRNA indicate changes in post-transcriptional processing of the microRNA. Pri-miR and pre-miR levels for miR-329, miR-487b, miR-494 and miR-495 showed no difference in expression levels between the GSO-treated groups. These data indicate that there is no direct transcriptional regulation by MEF2a of the 14q32 microRNAs studied here in this model and that the effects on mature miR-329 and miR-494 levels were achieved through other mechanism than transcription. Using RIP experiments, we demonstrated specific binding of MEF2A to the pri-miR-494 transcript, but not to pri-miR-487b, a microRNA that was not regulated by Mef2a inhibition in our study. As pri-miR-329 levels were too low in 3T3 cells, we could not confirm or exclude MEF2A binding. Nonetheless, we show here for the first time that MEF2A may not only function as transcription factor, but potentially also as RNA Binding Protein. Future experiments will have to determine whether MEF2A can regulate post-transcriptional processing of other 14q32 microRNAs as well as non-14q32 microRNAs. For example, a recent study demonstrated that MEF2A, via miR-143, regulates proliferation, migration and H_2O_2 induced senescence of vascular smooth muscle cells[21]. This work by Zhao et. al. indeed shows that MEF2A can also regulate expression of microRNAs outside the 14q32 gene cluster.

In the study by Snyder *et al.,* microarray analysis of injured muscle tissue from Mef2a knockout mice revealed downregulation of multiple microRNAs located on mouse chromosome 12F1 (14q32 in humans), indicating regulation of the 12F1/14q32 region by Mef2a, at least in response to injury[12]. To evaluate the role of Mef2a in skeletal muscle regeneration, the authors induced muscle injury in mice[12]. In our study, we made use of the hind limb ischemia model to investigate the role of Mef2a in post-ischemic neovascularization in which no direct damage to the muscle itself was introduced. Furthermore, Snyder *et al.* determined the expression of 14q32 microRNAs in (injured) muscle tissue of Mef2a knockout mice, whereas we measured expression of 14q32 microRNAs in C57Bl/6 muscle tissue wherein Mef2a expression was reduced by ~25% only using GSOs[12]. These differences in the chosen models may explain the observed discrepancies in the regulation of 14q32 microRNAs by Mef2a.

Following the improved blood flow recovery in GSO-Mef2a treated mice, we observed increased arteriogenesis in the adductor muscle of these mice. Phenotypic switching of SMCs, from a contractile to proliferative state, is an important processes in arteriogenesis and other forms of vascular remodelling[22]. Our results would imply that inhibition of Mef2a stimulates proliferation of SMCs, as GSO-Mef2a treated animals showed increased αSMA$^+$ collateral areas compared to GSO-Control treated mice. These findings are in line with the study of Zhao *et al.*, who reported increased proliferation and migration of human SMCs and downregulation of SMC markers upon MEF2A siRNA treatment[19]. Firulli *et al.* reported that the high levels of MEF2A expression in the neointima of rats upon balloon injury correlated with an activated SMC phenotype rather than a mere differentiated phenotype[18]. In addition, we observed increased angiogenesis in the ischemic soleus muscle of GSO-Mef2a treated animals. Collectively, our data suggest that Mef2a plays a role in SMC differentiation and proliferation as well as EC proliferation.

In conclusion, our study demonstrates a novel function for MEF2A in post-ischemic neovascularization and provides a link between MEF2A, 14q32 microRNAs miR-329 and miR-494 and arteriogenesis and angiogenesis. MEF2A acts a novel switch in vascular remodelling and neovascularization. Inhibition of MEF2A expression may be a promising therapeutic strategy to increase neovascularization and blood flow towards the extremities in patients with PAD.

Acknowledgements
We thank W. Razawy, W. Wong, T. Bezhaeva and C.M. Janssen for their technical support. We thank R.A. Boon for sharing the protocol on RNA binding protein immunoprecipitation. This work was supported by the Netherlands Institute for Regenerative Medicine (NIRM, FES0908), the Netherlands Organization for Scientific Research (NWO, Veni-916.12.041) and the Dutch Heart Foundation (Dr. E. Dekker Senior Postdoc, 2014T102).

References

1. van Oostrom MC, van Oostrom O., Quax PH, Verhaar MC, Hoefer IE. Insights into mechanisms behind arteriogenesis: what does the future hold? J Leukoc Biol. 2008;84:1379-1391.
2. Risau W. Mechanisms of angiogenesis. Nature. 1997;386:671-674.
3. Bartel,D.P. MicroRNAs: genomics, biogenesis, mechanism, and function. *Cell* **116**, 281-297 (2004).
4. van Rooij E. & Olson,E.N. MicroRNA therapeutics for cardiovascular disease: opportunities and obstacles. *Nat. Rev. Drug Discov.* **11**, 860-872 (2012).
5. Ono,K., Kuwabara,Y., & Han,J. MicroRNAs and cardiovascular diseases. *FEBS J.* **278**, 1619-1633 (2011).
6. Thum,T. & Condorelli,G. Long noncoding RNAs and microRNAs in cardiovascular pathophysiology. *Circ. Res.* **116**, 751-762 (2015).
7. Boon,R.A. & Dimmeler,S. MicroRNAs in myocardial infarction. *Nat. Rev. Cardiol.* **12**, 135-142 (2015).
8. Feinberg,M.W. & Moore,K.J. MicroRNA Regulation of Atherosclerosis. *Circ. Res.* **118**, 703-720 (2016).
9. Welten,S.M., Goossens,E.A., Quax,P.H., & Nossent,A.Y. The multifactorial nature of microRNAs in vascular remodel ling. *Cardiovasc. Res.*(2016).
10. Welten,S.M. *et al.* Inhibition of 14q32 MicroRNAs miR-329, miR-487b, miR-494, and miR-495 increases neovascular ization and blood flow recovery after ischemia. *Circ. Res.* **115**, 696-708 (2014).
11. Seitz,H. *et al.* A large imprinted microRNA gene cluster at the mouse Dlk1-Gtl2 domain. *Genome Res.* **14**, 1741-1748 (2004).
12. Snyder,C.M. *et al.* MEF2A regulates the Gtl2-Dio3 microRNA mega-cluster to modulate WNT signaling in skeletal muscle regeneration. *Development* **140**, 31-42 (2013).
13. Clark,A.L. & Naya,F.J. MicroRNAs in the Myocyte Enhancer Factor 2 (MEF2)-regulated Gtl2-Dio3 Noncoding RNA Locus Promote Cardiomyocyte Proliferation by Targeting the Transcriptional Coactivator Cited2. *J. Biol. Chem.* **290**, 23162-23172 (2015).
14. Fiore,R. *et al.* Mef2-mediated transcription of the miR379-410 cluster regulates activity-dependent dendritogenesis by fine-tuning Pumilio2 protein levels. *EMBO J.* **28**, 697-710 (2009).
15. Edmondson,D.G., Lyons,G.E., Martin,J.F., & Olson,E.N. Mef2 gene expression marks the cardiac and skeletal muscle lineages during mouse embryogenesis. *Development* **120**, 1251-1263 (1994).
16. Potthoff,M.J. & Olson,E.N. MEF2: a central regulator of diverse developmental programs. *Development* **134**, 4131-4140 (2007).
17. Hayashi,M. *et al.* Targeted deletion of BMK1/ERK5 in adult mice perturbs vascular integrity and leads to endothelial failure. *J. Clin. Invest* **113**, 1138-1148 (2004).
18. Firulli,A.B. *et al.* Myocyte enhancer binding factor-2 expression and activity in vascular smooth muscle cells. Associa tion with the activated phenotype. *Circ. Res.* **78**, 196-204 (1996).
19. Zhao,W., Zhao,S.P., & Peng,D.Q. The effects of myocyte enhancer factor 2A gene on the proliferation, migration and phenotype of vascular smooth muscle cells. *Cell Biochem. Funct.* **30**, 108-113 (2012).
20. Suzuki,E. *et al.* Myocyte enhancer factor 2 mediates vascular inflammation via the p38-dependent pathway. *Circ. Res.* **95**, 42-49 (2004).
21. Zhao,W., Zheng,X.L., Peng,D.Q., & Zhao,S.P. Myocyte Enhancer Factor 2A Regulates Hydrogen Peroxide-Induced Senescence of Vascular Smooth Muscle Cells Via microRNA-143. *J. Cell Physiol* **230**, 2202-2211 (2015).
22. Schirmer,S.H., van Nooijen,F.C., Piek,J.J., & van,R.N. Stimulation of collateral artery growth: travelling further down the road to clinical application. *Heart* **95**, 191-197 (2009).
23. Bhagat,L. *et al.* Novel oligonucleotides containing two 3'-ends complementary to target mRNA show optimal gene-silencing activity. *J. Med. Chem.* **54**, 3027-3036 (2011).
24. Hellingman,A.A. *et al.* Variations in surgical procedures for hind limb ischaemia mouse models result in differences in collateral formation. *Eur. J. Vasc. Endovasc. Surg.* **40**, 796-803 (2010).
25. Nossent,A.Y. *et al.* The 14q32 microRNA-487b targets the antiapoptotic insulin receptor substrate 1 in hypertension-induced remodeling of the aorta. *Ann. Surg.* **258**, 743-751 (2013).
26. Bastiaansen,A.J. *et al.* TLR4 accessory molecule RP105 (CD180) regulates monocyte-driven arteriogenesis in a murine hind limb ischemia model. *PLoS. One.* **9**, e99882 (2014).
27. Baker,M. *et al.* Use of the mouse aortic ring assay to study angiogenesis. *Nat. Protoc.* **7**, 89-104 (2012).

Supplemental Material

Gene	Forward Primer	Reverse Primer
primiR-329	AAGGTCACGTTGGGGAATTA	ACCACGAAGCCTCCAAGAT
premiR-329	TGGTACCGGAAGAGAGGTTTT	AGGTTAGCTGGGTGTGTTTCA
primiR-487b	CTGAGGCGGTGGCTTTG	GAAGCCAGGCTGCAGAGTC
premiR-487b	TGTCCTCTTCGCTTCACTCA	TGAAAAAGTGGATGACCCTGT
primiR-494	TGCCTTTGTTTGCTTTCTGA	GTCATCAGGGACAGGGAGTG
premiR-494	GGAGAGGTTGTCCGTGTTGT	AGGTTTCCCGTGTATGTTTCA
primiR-495	AGCATCCCTTCACACTCAGG	GAGCTCTCCAAGGTGAGATTTG
premiR-495	GTTGCCCATGTTATTTTTCG	AGTGCACCATGTTTGTTTCG

Supplementary Table 1. List of primers used for primiR and premiR quantification.

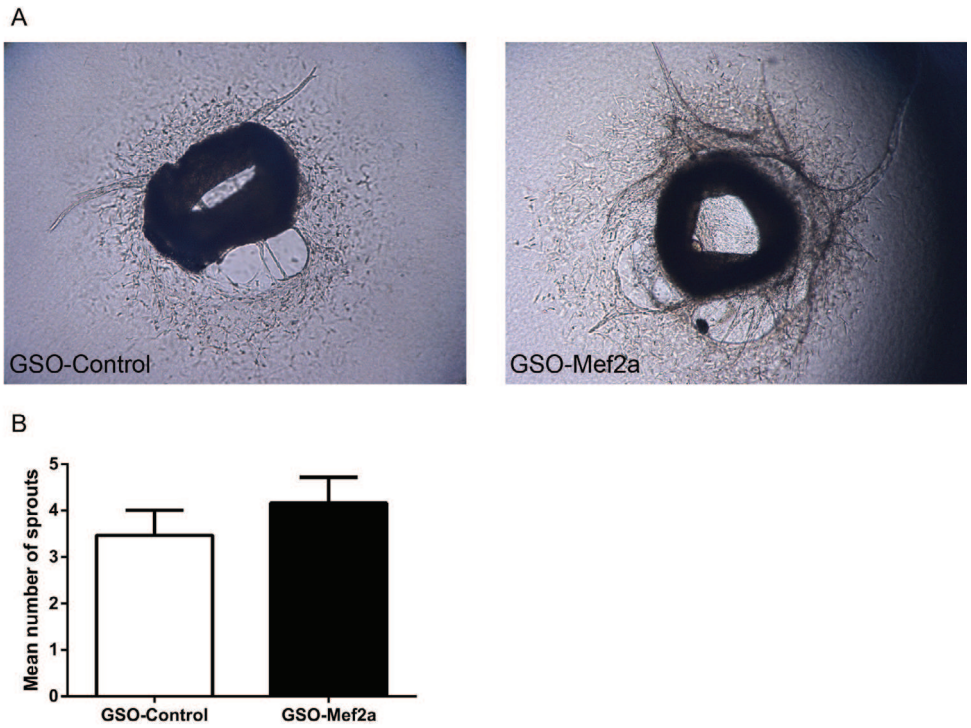

Supplemental Figure 1. Ex vivo sprouting angiogenesis. (A) Outgrowth of neovessels from 5-day collagen-embedded aortic rings treated with GSO-Control or GSO-Mef2a. **(B)** Quantification of neovessels. Data are presented as mean ± SEM and represent 3 independent experiments with 10 rings per condition.